Tunable Assembly of Organosilica Hollow Nanospheres

Jian Liu,[†] Shiyang Bai,[†,‡] Hua Zhong,[†] Can Li,*[,†] and Qihua Yang*[,†]

State Key Laboratory of Catalysis, Dalian Institute of Chemical Physics, Chinese Academy of Sciences, 457 Zhongshan Road, Dalian 116023, China, and Graduate School of the Chinese Academy of Sciences, Beijing 100049, China

Received: October 16, 2009; Revised Manuscript Received: December 1, 2009

Hollow nanospheres with a particle size of less than 25 nm have been successfully fabricated using an ethylene-, phenylene-, and 1,4-diethylphenylene-bridging silane precursor with F127 as a soft template under an acidic medium. As the size and flexibility of the bridging organic group increases, it is more and more difficult for the formation of hollow nanospheres. The organic additive, 1,3,5-trimethylbenzene, could finely tune the particle size of the nanosphere from 12 to 25 nm. It was found that silane precursors with hydrophobicity and slow hydrolysis rate favor the formation of hollow nanospheres and hydrophilic silane precursors such as tetramethoxysilane induce the formation of mesostructured bulk materials. Under the current synthesis conditions, carefully tuning the interaction between templates and silica species, organosilica hollow nanospheres with controlled composition can be successfully obtained.

1. Introduction

There has been growing interest in the past decade in frabricating organosilicas with various nanostructures, such as nanospheres, nanowires, nanotubes/nanorods, and nanoporous structures (e.g., periodic mesoporous organosilicas), etc., owing to their potential applications in catalysis, therapeutics, and optical and electronic devices.[1–5] A typical and important class of organosilica nanostructures is hollow nanospheres.[5] Compared with silica hollow nanospheres, organosilica hollow nanospheres (OHNs) combine the advantages of organic domains and inorganic building blocks and they are more easily modified through chemical transformation of the organic groups in the hybrid framework. The fabrication of organosilicas in nanospherical morphology has attracted much research attention because of their potential applications in catalysis, drug delivery, and protection materials for biomolecules.[5–11]

Due to the difficulty in the synthesis of hollow nanospheres, there are only limited reports for the synthesis of OHNs.[5–11] The first OHNs (particle size in the range 300−800 nm) with ethylene-bridging group and highly ordered mesoporous structure in the shell were reported by Lu's group through a vesicle and a liquid crystal "dual templating" approach.[5] Recently, the ethane−silica hollow nanospheres were facilely synthesized through condensation of 1,2-bis(trimethoxysilyl)ethane (BTME) around an inorganic-electrolyte-stabilized F127 micelle under mild buffer conditions (NaH_2PO_4−Na_2HPO_4, pH ≈ 7.0).[6] Multilamellar vesicles, ethane−silica hollow nanoparticles, were also synthesized using a cationic surfactant with a partially fluorinated tail.[7] The same method was extended for the synthesis of organosilica hollow particles using a silane precursor with a long bridging chain, such as bis(triethoxysilyl)octane, but only a limited number of particles have hollow spherical morphology.[7] Yu and co-workers reported the synthesis of multilamellar vesicles through a single-templating approach by using Pluronic P85 ($EO_{26}PO_{39}EO_{26}$) as a structure directing agent and 1,2-bis(triethoxysilyl)ethane as an organosilica source under mild conditions (pH 5.5).[9] The organosilica hollow spheres ever reported are mainly composed of ethylene bridging groups. Expanding the chemical composition of OHNs, which is one of the important factors determining their applications, is highly desirable.[12–15]

Though the synthesis of organosilica hollow particles with short bridging organic groups has been reported, the incorporation of large and flexible bridging organic groups in the hollow particle still remains a challenge due to the complex interactions of the bridging organic group with the surfactant micelles and the difficulty in forming the flexible network. In this paper, we report the successful synthesis of OHNs with ethylene, phenylene, and 1,4-diethylphenylene bridging groups in the network using F127 block copolymer micelles as a soft template under acidic conditions. It was found that the hydrophobicity/hydrophilicity of the silane precursor played an important role in the structure and morphology formation of the organosilicas.

2. Experimental Section

2.1. Chemicals and Reagents. Triblock poly(ethylene oxide)-*b*-poly(propylene oxide)-*b*-poly(ethylene oxide) copolymer $EO_{106}PO_{70}EO_{106}$ (Pluronic F127, M_w = 12600) and 1,2-bis(trimethoxysilyl)ethane (BTME, 96%) were purchased from Sigma-Aldrich Company Ltd. (U.S.A.). 1,4-Bis(trimethoxysilylethyl)benzene (BTSEB) was purchased from Gelest. Tetramethoxysilane (99%, TMOS), tetraethoxysilane (99%, TEOS), and other reagents were obtained from Shanghai Chemical Reagent, Inc., of Chinese Medicine Group. All materials were analytical grade and used without any further purification. 1,4-Bis(triethoxysilyl)benzene (BTEB) was synthesized according to the literature.[16]

2.2. Synthetic Procedure. ***2.2.1. Synthesis of Organosilica Hollow Nanospheres and Mesoporous Organosilicas with Different Bridging Groups.*** In a typical synthesis, 1.0 g of F127, the desired amount of 1,3,5-trimethylbenzene (TMB) (TMB = 0, 0.5, 1.0, 2.0 g), and KCl (KCl = 0, 2.5, 5.0, 10.0 g) were

* To whom correspondence should be addressed. E-mail: yangqh@dicp.ac.cn (Q.Y.); canli@dicp.ac.cn (C.L.). Phone: 86-411-84379552 (Q.Y.); 86-411-84379070 (C.L.). Fax: 86-411-84694447. URL: http://www.hmm.dicp.ac.cn (Q.Y.); http://www.canli.dicp.ac.cn (C.L.).

† Dalian Institute of Chemical Physics, Chinese Academy of Sciences.

‡ Graduate School of the Chinese Academy of Sciences.

10.1021/jp909931z
Published on Web 12/22/2009

TABLE 1: Preparation Parameters and Physicochemical Properties of Nanostructured Ethane−Silicas (NES-0-*b*)

sample	KCl/F127 molar ratio	TMB/F127 molar ratio	BET surface area (m^2 g^{-1})	cavity diameter (nm)	shell thickness[a] (nm)	total pore volume (cm^3 g^{-1})
NES-0-0	0	0	872	3.8[b] (6)[c]	3	2.89
NES-0-105	0	105	730	14.4[b] (15)[c]	5	2.42
NES-0-210	0	210	885	8.7[b] (12)[c]	4	2.93

[a] Shell thickness is estimated by TEM analysis. [b] Cavity diameter is calculated by the BJH method of pore size distribution. [c] The cavity diameter estimated by TEM analysis is in parentheses.

TABLE 2: Preparation Parameters and Physicochemical Properties of Nanostructured Benzene−Silicas (NBS-*a*-105)

sample	KCl/F127 molar ratio	TMB/F127 molar ratio	BET surface area (m^2 g^{-1})	cavity diameter (nm)	shell thickness[a] (nm)	total pore volume (cm^3 g^{-1})
NBS-0-105	0	105	471	6.6[b] (7)[c]	5.5	1.48
NBS-423-105	423	105	594	5.5[b] (7)[c]	5.5	2.00
NBS-846-105	846	105	600	7.2[b] (7)[c]	5	1.99
NBS-1691-105	1691	105	562	7.2[b] (7)[c]	4.5	1.53

[a] Shell thickness is estimated by TEM analysis. [b] Cavity diameter is calculated by the BJH method of pore size distribution. [c] The cavity diameter estimated by TEM analysis is in parentheses.

dissolved in 60 mL of 2 M HCl at 40 °C under vigorous stirring. When the copolymer was fully dissolved, 10 mmol of organosilane precursor was added under stirring. The resultant mixture was stirred at the same temperature for 24 h and aged at 100 °C under static conditions for an additional 24 h. The solid product was recovered by filtration and air-dried at room temperature overnight. Finally, the surfactant was extracted by refluxing 1.0 g of as-synthesized material in 200 mL of ethanol containing 1.5 g of concentrated aqueous HCl solution for 24 h. The surfactant-free sample synthesized using BTME, BTEB, and BTSEB was denoted as NES-*a*-*b*, NBS-*a*-*b*, and NBSB-*a*-*b*, respectively, where *a* is the molar ratio of KCl/F127 and *b* is the molar ratio of TMB/F127. The molar ratio of the reactants is F127/organosilane precursor/TMB/KCl/HCl/H_2O = 1:313:(0−210):(0−1692):1884:52326, as listed in Tables 1 and 2 and Table S1 in the Supporting Information.

2.2.2. Synthesis of Silica Particles Using TMOS, and TEOS as the Silane Source. The synthesis method was similar to that for the synthesis of organosilicas mentioned above but using TMOS (20 mmol) or TEOS (20 mmol) as the silane precursor. The surfactant-free sample synthesized using TMOS and TEOS as the silane precursor was denoted as NTM-*a*-*b* and NTE-*a*-*b* (*a* is the molar ratio of KCl/F127, and *b* is the molar ratio of TMB/F127), respectively. The molar ratio of the reactants is F127/Si/TMB/KCl/HCl/H_2O = 1:626:423:(0−105):1884:52326, as listed in Table S1 of the Supporting Information.

2.3. Characterization. X-ray diffraction (XRD) patterns were recorded on a Rigaku RINT D/Max-2500 powder diffraction system using Cu Kα radiation of 0.15406 nm wavelength. The nitrogen sorption experiment was performed at 77 K on a Micromeritics ASAP 2020 system. Prior to the measurement, the samples were outgassed at 120 °C for at least 6 h. The Brunauer−Emmett−Teller (BET) specific surface areas were calculated using adsorption data at the relative pressure range of P/P_0 = 0.05−0.25. Pore size distributions were calculated from the adsorption branch using the Barrett−Joyner−Halenda (BJH) method. The total pore volumes were estimated from the amount adsorbed at a relative pressure (P/P_0) of 0.99. Field-emission scanning electron microscopy (FESEM) was undertaken on a HITACHI S-4800 microscope operating at an accelerating voltage of 1−30 kV. Transmission electron microscopy (TEM) was performed using a FEI Tecnai G^2 Spirit at an acceleration voltage of 120 kV. FT-IR spectra were collected with a Nicolet Nexus 470 IR spectrometer with KBr pellet. ^{13}C (100.5 MHz) cross-polarization magic angle spinning (CP-MAS) and ^{29}Si (79.4 MHz) MAS solid-state NMR experiments were recorded on a Varian infinity-plus 400 spectrometer equipped with a magic angle spin probe in a 4-mm ZrO_2 rotor. ^{13}C and ^{29}Si signals were referenced to tetramethylsilane. The experimental parameters were 8 kHz spin rate, 3 s pulse delay, 4 min contact time, and 1500−3000 scans for ^{13}C CP-MAS NMR experiments and 4 kHz spin rate, 180 s pulse delay, 10 min contact time, and 116 scans for ^{29}Si MAS NMR experiments.

3. Results and Discussion

3.1. Results. ***3.1.1. Synthesis of Ethane−Silica Hollow Nanospheres with Tunable Particle Sizes.*** NES-0-*b* samples were prepared using F127 triblock copolymer template in the presence of different amounts of TMB under acidic conditions. NES-0-0 synthesized in the absence of TMB is composed of aggregated hollow nanospheres (Figure 1a). The TEM images of NES-0-*b* (*b* = 105, 210) synthesized with the addition of TMB show the existence of monodispersed hollow nanospheres, suggesting that the addition of TMB could increase the dispersion degree of the hollow nanospheres (Figure 1b). The SEM image of NES-0-105 (Figure 1c) reveals that this sample indeed has spherical morphology with a particle size of ∼25 nm. With the TMB/F127 molar ratio increasing from 0 to 105, the particle size of the hollow nanospheres increases from 12 to 25 nm accompanied with the size of the hollow cage increasing from 6 to 15 nm, implying that TMB could act as a swelling agent to penetrate into the core of micelles formed by $EO_{106}PO_{70}EO_{106}$ (F127) copolymers. The particle size of the hollow nanospheres decreases to 20 nm when the TMB/F127 molar ratio is increased to 210 (Figure 1d). The above results exhibit that TMB not only helps the formation of monodispersed hollow nanospheres but also can be used to finely tune the particle and core size of the hollow nanospheres.

N_2 adsorption−desorption isotherms and pore size distributions of NES-0-*b* (synthesized with different TMB/F127 molar ratios) are presented in Figure 2. All samples show type IV isotherms with two hysteresis loops at the relative pressures P/P_0 = 0.45−0.85 and P/P_0 = 0.8−0.9, which is from the hollow cage and void space between the nanoparticles, respectively. With the TMB/F127 molar ratio increasing from 0 to 105 and to 210, the cage size increases from 3.8 to 14.4 nm

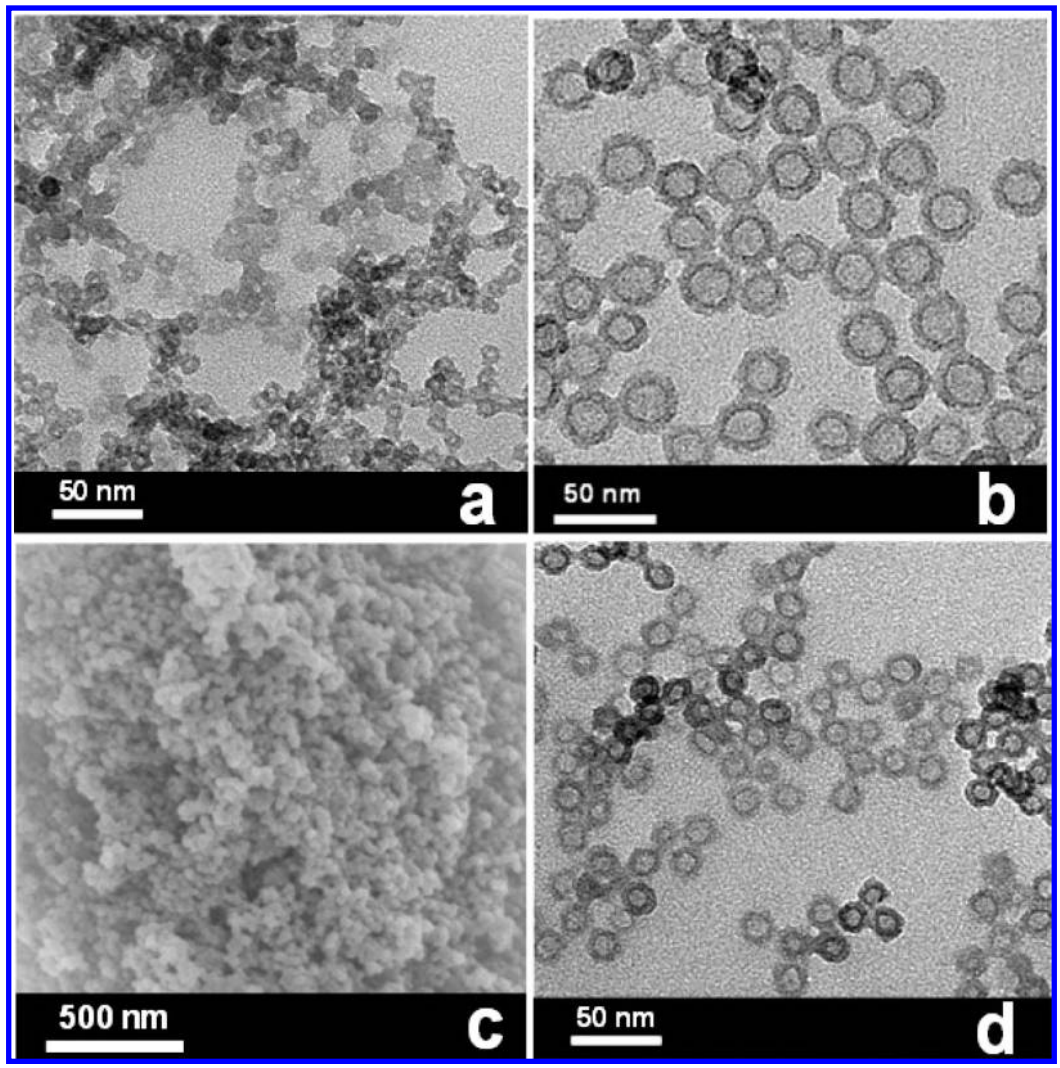

Figure 1. Representative TEM (a, c, d) and SEM (b) images of organosilica hollow nanospheres NES-0-*b* synthesized with different molar ratios of TMB/F127: (a) TMB/F127 = 0, (b, c) TMB/F127 = 105, (d) TMB/F127 = 210.

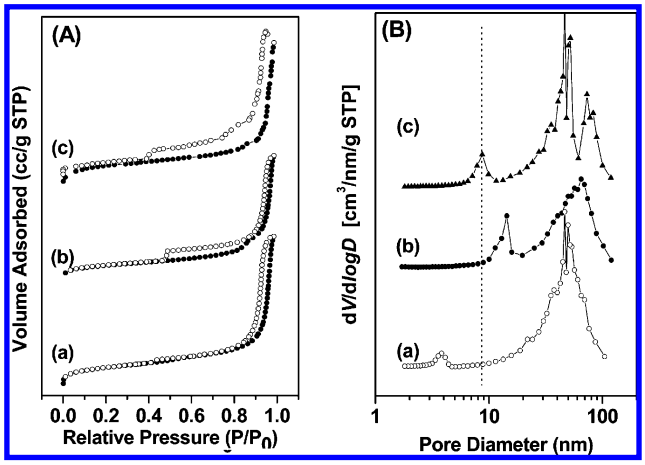

Figure 2. Nitrogen adsorption (●) and desorption (○) isotherm curves (A) and pore size distributions (B) of organosilica hollow nanospheres NES-0-*b* synthesized with different molar ratios of TMB/F127: (a) TMB/F127 = 0, (b) TMB/F127 = 105, (c) TMB/F127 = 210.

and then decreases to 8.7 nm, which is consistent with the results of the TEM (Figure 2B and Table 1). The difference of the cage size calculated from the BJH and estimated from the TEM is mainly due to the fact that the BJH model is not very suitable for determining the pore size with cage structure.[11,17] All of the samples show high BET surface areas (730−885 $m^2\ g^{-1}$) and large pore volumes (2.42−2.98 $cm^3\ g^{-1}$) (Table 1).

3.1.2. Incorporation of Phenylene and 1,4-Diethylphenylene into the Hollow Sphere. Phenylene has been fused into the mesoporous organosilicas under either acid or base medium.[18–20] Compared with the ethylene group, the phenylene is more reactive toward chemical reactions, such as sulfonation, alkylation, nitration, etc.[21–23] However, the structure and morphology control of the organosilicas with bridging phenylene group is not fully investigated. NBS-0-105 was synthesized using 1,4-bis(triethoxysilyl)benzene (BTEB) as the silane precursor under similar conditions to NES-0-105. The TEM image of NBS-0-105 shows that this sample is composed of aggregated hollow nanospheres with a particle size of of ∼18 nm and shell thickness of ∼5.5 nm (Figure 3a and Table 2). Compared with BTME, BTEB is more hydrophobic. The different hydrophobicity of the silane precursor may have a big influence on the structure and morphology of the resultant materials. In order to optimize the dispersion degree and particle size of the benzene−silica hollow nanosphere, KCl was added in the initial mixture because the inorganic salts were always used to adjust the structure and morphology of the mesoporous materials in combination with nonionic copolymer surfactant.[24,25] The TEM

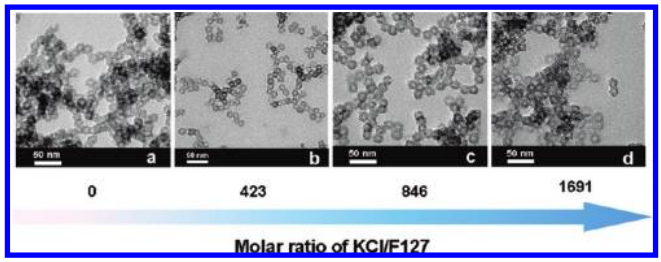

Figure 3. TEM images of organosilica hollow nanospheres NBS-*a*-105 synthesized with different molar ratios of KCl/F127: (a) KCl/F127 = 0, (b) KCl/F127 = 423, (c) KCl/F127 = 846, (d) KCl/F127 = 1692.

images of NBS-*a*-105 synthesized with different KCl concentrations are displayed in Figure 3. The well dispersed hollow nanopheres are clearly observed in the TEM images of NBS-423-105 and NBS-846-105. However, higher KCl concentration results in aggregated hollow nanospheres, as evidenced by the TEM image of NBS-1692-105. The particle size of NBS-423-105, NBS-846-105, and NBS-1692-105 is about 18 nm. The SEM image of NBS-423-105 (Figure S1, Supporting Information) shows the existence of fused nanospheres, further confirming that NBS samples have hollow nanosphere morphology.

The effect of KCl on the morphology formation of NES samples was also investigated (Table S1, Supporting Information). With the molar ratio of KCl/F127 in the range 0−846, all of the NES samples have hollow nanospherical morphology, though the dispersion degree of the hollow nanospheres decreases as the amount of KCl increases (Figures S2a−c, Supporting Information). It is worth mentioning that NES-1691-105 (Figure S2d, Supporting Information) is mainly composed of mesostructured bulk materials, which is quite different from NBS-1691-105 with hollow nanospherical morphology. The different morphology of NES-1691-105 and NBS-1691-105 is probably due to the different hydrolysis and condensation rate between BTME and BTEB.

NBSB-423-105 was synthesized using 1,4-bis(trimethoxysilylethyl)benzene (BTSEB) as the silane precursor. To our delight, hollow nanospheres could still be observed in the TEM image of NBSB-423-105, though the contrast between the core and shell is not as clear as that of NES and NBS samples. The particle size is ∼16 nm estimated from the TEM image (Figure 4).

Similar to NES samples, the N_2 adsorption−desorption isotherm of all NBS samples show type IV isotherms with two hysteresis loops (Figure 5). Compared with NES samples, the first hysteresis loop at relative pressure P/P_0 is rather small. Moreover, all NBS samples show much lower BET surface area (471−600 $m^2\ g^{-1}$) and pore volume (1.48−2.00 $cm^3\ g^{-1}$) than NES samples (Table 2). The BET surface area and pore volume of NBSB-423-105 are 157 $m^2\ g^{-1}$ and 0.18 $cm^3\ g^{-1}$, respectively.

From the above results, we could see that the F127-TMB-HCl system is very efficient for the synthesis of OHNs with either short or long flexible organic bridging groups.

3.1.3. Synthesis of Silica Particles Using TEOS or TMOS as the Precursor. The F127-TMB-HCl system is very effective for the synthesis of organosilica hollow nanospheres using different kinds of organosilane precursors. For further investigating the generality of this method and understanding the synthetic mechanism, NTM and NTE samples were synthesized under similar conditions to organosilica nanospheres but using TMOS and TEOS as the silane precursor, respectively. The XRD pattern of NTM-0-105 shown in Figure 6a displays one sharp diffraction peak, indicating that this sample has less ordered mesoporous structure. The nitrogen sorption isotherm of NTM-0-105 is of type IV with an H3 hysteresis loop (Figure 6b), implying that this sample has a mesostructure similar to FDU-12 with a cage-like pore connected by windows with a small size.[24] TEM images of NTM-0-105 mainly show the coexistence of wormlike and cubic mesostructure (Figure 6c). A sharp diffraction peak can be clearly observed in the low angle region in the XRD pattern of NTE-0-105, which is synthesized using TEOS as the precursor (Figure 7a). The nitrogen adsorption−desorption isotherm of NTE-0-105 shows a two-step uptake in the adsorption isotherm (Figure 7b). The first uptake at P/P_0 with an H3 hysteresis loop, characteristic of cage-like mesostructure, is probably from disordered mesostructure and the cage of the hollow nanospheres. The second uptake at a relative pressure P/P_0 of 0.85−1.00 is probably from the void space among the aggregated hollow nanospheres. NTE-0-105 is composed of the aggregated hollow nanospheres (with a size of ∼14 nm) and particles with wormhole-like mesostructure (Figure 7c).

NES-0-105, NBS-0-105, NTM-0-105, and NTE-0-105 samples were synthesized under similar conditions but using different kinds of silane precursors. However, the morphology of these samples is quite different. NES-0-105 and NBS-0-105 have nanospherical morphology. NTM-0-105 and NTE-0-105 are mainly composed of the mesostructured particles and the coexistence of hollow nanospheres and the mesostructured particles, respectively.

The effect of KCl on the morphology and structure formation of NTM and NTE samples was also investigated. NTM-423-105 and NTE-423-105 (FDU-12) synthesized with the addition of KCl both have highly ordered FDU-12-type mesostructure (Figures S3 and S4, Supporting Information). Under similar conditions, NES-423-105 and NBS-423-105 have nanospherical morphology. In combination with the above results, it can be concluded that the silane precursor plays an important role in the morphology formation. Scheme 1 summarizes the relation between the morphology and the kind of silane precursors.

3.1.4. Characterization of the Chemical Composition of the OHNs. The chemical composition of different kinds of OHNs was characterized by FT-IR spectroscopy. The FT-IR spectra of representative samples, NES-0-105 and NBS-423-105, are summarized in Figure S5 of the Supporting Information. The C−H vibrations of $-CH_2CH_2-$ appear in the range 2918−2875 cm^{-1} and at 1160 cm^{-1} are clearly observed in the FT-IR spectrum of NES-0-105. The FT-IR spectrum of NBS-423-105 displays absorption bands attributed to the stretching modes of C−H species (3010−3060 cm^{-1}) and the overtones of benzene ring vibrations (1300−2000 cm^{-1}). The FT-IR spectra of these two samples clearly show the Si−C stretching modes at 696 and 768 cm^{-1}, proving the integrity of the organic groups in the OHNs. The C−H vibrations of the surfactant at 1272, 1412, 2890, and 2895 cm^{-1} are quite weak, demonstrating that most surfactant could be removed during the extraction process.

The solid-state NMR analysis was performed to further verify the composition of the OHNs. The resonance at 5.8 ppm in the ^{13}C NMR spectrum of NES-0-105 is due to the C species of the ethane moiety (Figure 8a). The ^{13}C NMR spectrum of NBS-423-105 displays the signal of a benzene moiety at 133.9 ppm (Figure 8b). The signals at 70.5, 58.5, and 16.3 ppm are due to the residue surfactants and the carbons of the ethoxy groups formed during the surfactant extraction process. Considering the hollow structure, it is reasonable to observe the existence of an ethanol residue in the hollow cage of the final materials. Moreover, extraction of the F127 with ethanol also generates

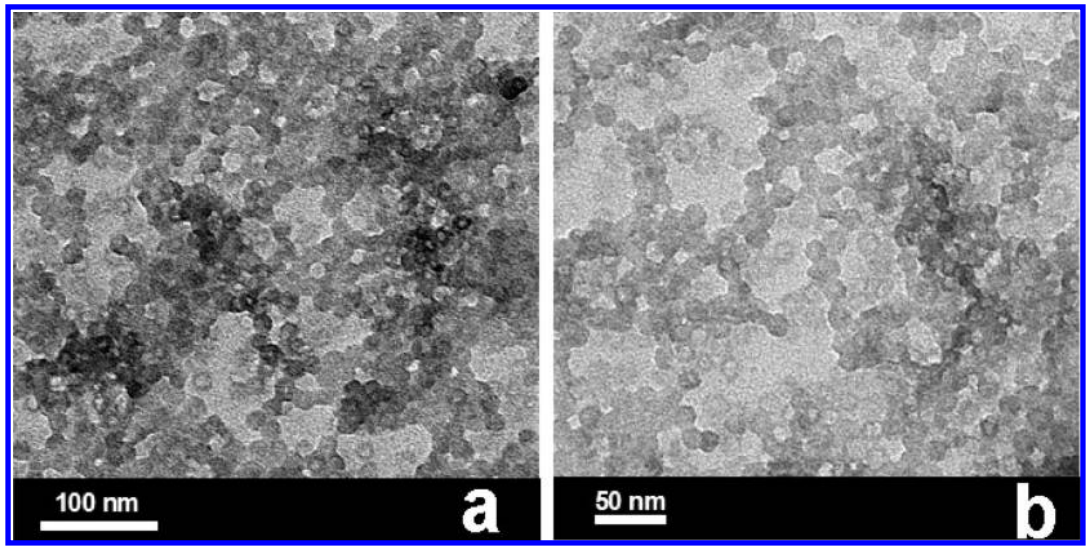

Figure 4. TEM images of nanostructured silica NBSB-423-105 synthesized using BTSEB as the silica precursor with different magnifications: (a) low magnification, (b) high magnification.

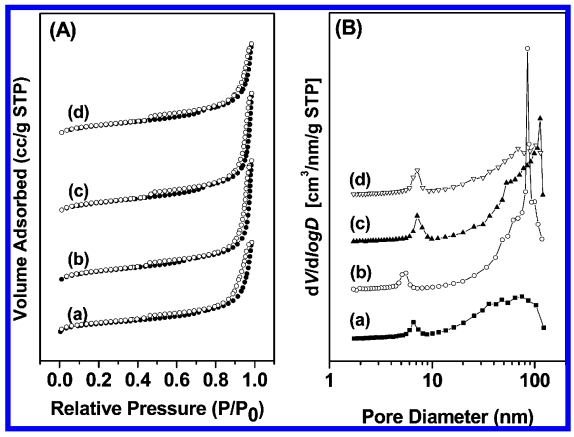

Figure 5. Nitrogen adsorption (●) and desorption (○) isotherm curves (A) and pore size distributions (B) of organosilica hollow nanospheres NBS-*a*-105 synthesized with different molar ratios of KCl/F127: (a) KCl/F127 = 0, (b) KCl/F127 = 423, (c) KCl/F127 = 846, (d) KCl/F127 = 1692.

some ethoxy groups through the reaction of ethanol with the silanol groups. The result of solid-state ^{13}C CP MAS NMR confirmed the incorporation and integrity of ethylene and phenylene groups in the hollow spheres.

^{29}Si NMR spectra of NES-0-105 and NBS-423-105 show the existence of ^{n}T sites as expected (Figure 9). The signals at −61.3, −70.7, and −73.7 ppm for NES-0-105 and the signals at −74.3, −81.9, and −88.7 ppm for NBS-423-105, assigned to T^1 [$SiC(OH)_2(OSi)$], T^2 [$SiC(OH)(OSi)_2$], and T^3 [$SiC(OSi)_3$], respectively, confirm the full framework linkage of the organosilica hollow nanospheres. The absence of SiO_4 species such as Q^3 [$Si(OH)(OSi)_3$] and Q^4 [$Si(OSi)_4$] in the range of −90 to −120 ppm confirms that no carbon−silicon bond cleavage occurred during the synthesis of the hollow nanospheres.

The combined results of NMR and FT-IR analysis confirm the OHNs are composed of $O_{1.5}Si-R-SiO_{1.5}$ units.

3.2. Discussion. ***3.2.1. Effect of the Silane Precursor on the Formation of Hollow Nanospheres.*** From NES to NBS and to NBSB, the BET surface area and pore volume decrease and the formation of the nanospheres becomes more and more difficult. The size and flexibility of the organic group increase in the order of ethylene > phenylene >1,4-diethylphenylene. Therefore, it is more difficult for the structure and morphology control of the organosilicas as the precursor is shifted from BTME to BTSEB.[26–28] The above differences in the morphology and the BET surface area of NES, NBS, and NBSB samples may be partly from the larger size of phenylene than that of ethylene and partly from different induction and steric effects between ethylene and phenylene groups, which usually have a big influence on the sol−gel process of the silane precursors.[26]

The hollow nanospheres can be obtained using organosilane precursors, such as BTME, BTEB, and BTSEB. TMOS and TEOS induce the formation of mesostructured bulk materials and mixture of hollow nanospheres and mesostructured bulk materials, respectively. The different influence of the silane precursor on the morphology and structure formation may be due to the following factors: (1) The hydrophobicity/hydrophilicity of the silane precursors. This difference may influence the interaction between silicate precursors and templates that are amphiphilic in aqueous solution which resulted in different morphologies and structures. Generally, the hydrophobicity of the silane precursors decreases in the order of BTEB > BTME > TEOS > TMOS. The hydrophobic unhydrolyzed silica species could help F127 to form single micelles or nanoemulsions, thus acting as templates for the hollow nanospheres. As we mentioned above, the addition of organic additives such as TMB could help the formation of monodispersed hollow nanospheres. Therefore, the hollow nanospheres can be more easily obtained by using silane precursors with more hydrophobic properties, such as BTME, BTEB, and BTSEB. (2) The reactivity (hydrolysis/condensation rate) of the silane precursors. As the bulkiness of the alkoxide group increases, the hydrolysis and condensation rate decrease. With the consideration of the expected inductive and steric factors of the silanes,[26,29–32] the hydrolysis and condensation rate should decrease in the sequence of TMOS > TEOS > BTME > BTEB.[29–32] In the current sol−gel process, the nanostructured materials are formed as a result of the coassembly process between hydrolyzed silica species and the template. This sol−gel process is highly dependent on the availability of hydrolyzed silica species for coassembly. The silane precursor with fast hydrolysis rate can generate more hydrolyzed silica species to condense around the single micelles or nanoemulsion, which may lead to the formation of meso-

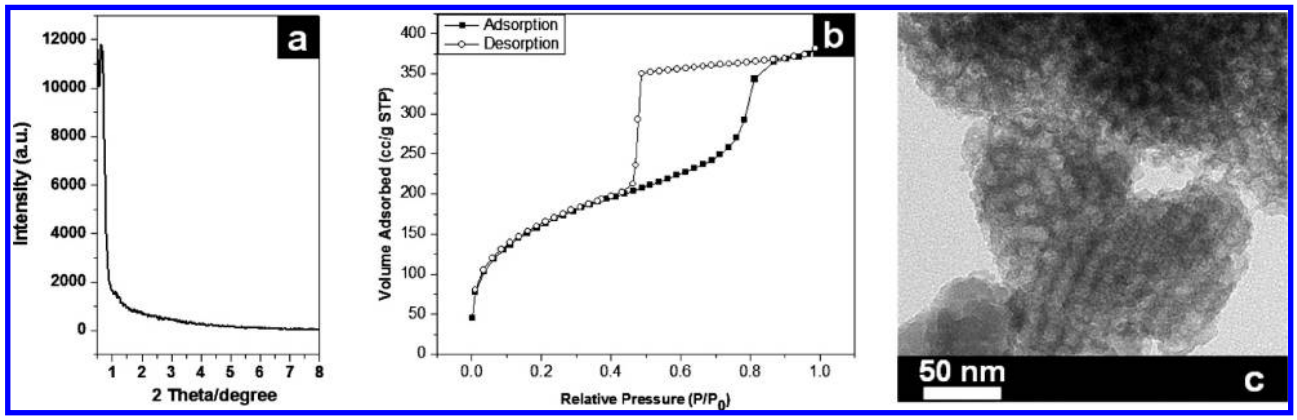

Figure 6. XRD pattern (a), nitrogen adsorption and desorption isotherm curves (b), and TEM images (c) of mesoporous silica NTM-0-105 synthesized using TMOS as the silica precursor.

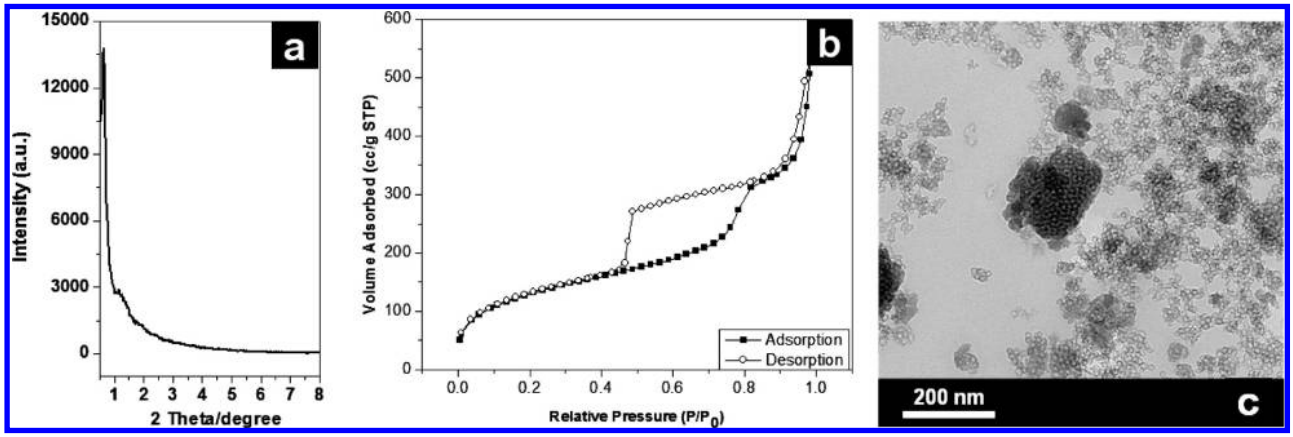

Figure 7. XRD pattern (a), nitrogen adsorption and desorption isotherm curves (b), and TEM images (c) of mesoporous silica NTE-0-105 synthesized using TEOS as the silica precursor.

structured particles. Therefore, TMOS with a fast hydrolysis rate among the silane precursors investigated leads to the formation of mesostructured particles. TEOS with a slower hydrolysis rate than TMOS tends to form the mixture of hollow nanospheres and the mesostructured particles. The hollow nanospheres could be easily formed by using organosilane precursors which have a slower hydrolysis rate than TMOS and TEOS.

3.2.2. Effect of Inorganic Salts (KCl) on the Formation of Hollow Nanospheres. The role of inorganic salts in the formation of silicas by using TMOS, TEOS, BTME, and BETB as the silane precursor is investigated. As the amount of KCl increases, the tendency to form aggregated particles increases no matter what kind of silane precursor is employed, suggesting that KCl can increase the reactivity of the silane precursor to condense around the surfactant micelles. The following factors may explain the roles of KCl played in the current synthesis system: (1) It can decrease the critical micelle concentration (CMC) of F127. (2) It can decrease the thermodynamic radius of micelles. (3) It can cause dehydration of ethylene oxide units from the hydrated PEO shell remaining adjacent to the PPO core, which leads to an increase in the hydrophobicity of the PPO moieties and a reduction in the hydrophilicity of the PEO moieties.[33–35] With the addition of KCl, the low-hydrophilic PEO head groups in the positively charged surfactant are expected to have increased interactions with the positively charged silica species. The strong interactions thus result in ordered cubic mesostructure by using TMOS, TEOS, and BTME as the silane source (Figures S2d, S3, and S4, Supporting Information). On the other hand, the salting-out effect of KCl will compete for water to interact with the PEO group, thus markedly causing the dehydration of F127 surfactant, which can lower the solubility of F127 and hence reduce its critical micelle concentration (CMC). This favors the micelle−micelle interaction and subsequently boosts the assembly ability of the micelles to generate the ordered mesostructure. Moreover, the hard sphere packing mechanism shows that face-centered cubic mesostructures can be packed by hollow nanospheres as building units through the strong interaction induced by inorganic salts.[36] Therefore, the combined effects of KCl favor the formation of aggregated hollow nanospheres or ordered mesoporous structure. The fact that BTEB cannot lead to the formation of ordered mesostructure even at high inorganic salt concentration may be explained by the disturbing effect of the large phenylene bridging group.

3.2.3. Effect of Organic Additive (TMB) on the Formation of Hollow Nanospheres. As we mentioned in part 3.1.1, the presence of TMB could help the formation of monodispersed hollow nanospheres and the amount of organic additive TMB plays an important role in determining the particle size and dispersing degree of the hollow nanospheres. It is reported that hydrophobic TMB molecules can dissolve in the core (PPO block) of micelles as a swelling agent to expand micelles.[24,25,35] Thus, the particle size of OHNs could be enlarged by addition of a different amount of TMB. The organic additives, which have a big influence on the hydrophobic properties of triblock copolymers, can also affect the quality and kinetic features of the self-assembly process. When TMB was added, the charge

SCHEME 1: Schematic Illustration of the Formation Mechanism of OHNs and the Relation between the Morphology and the Silane Precursors

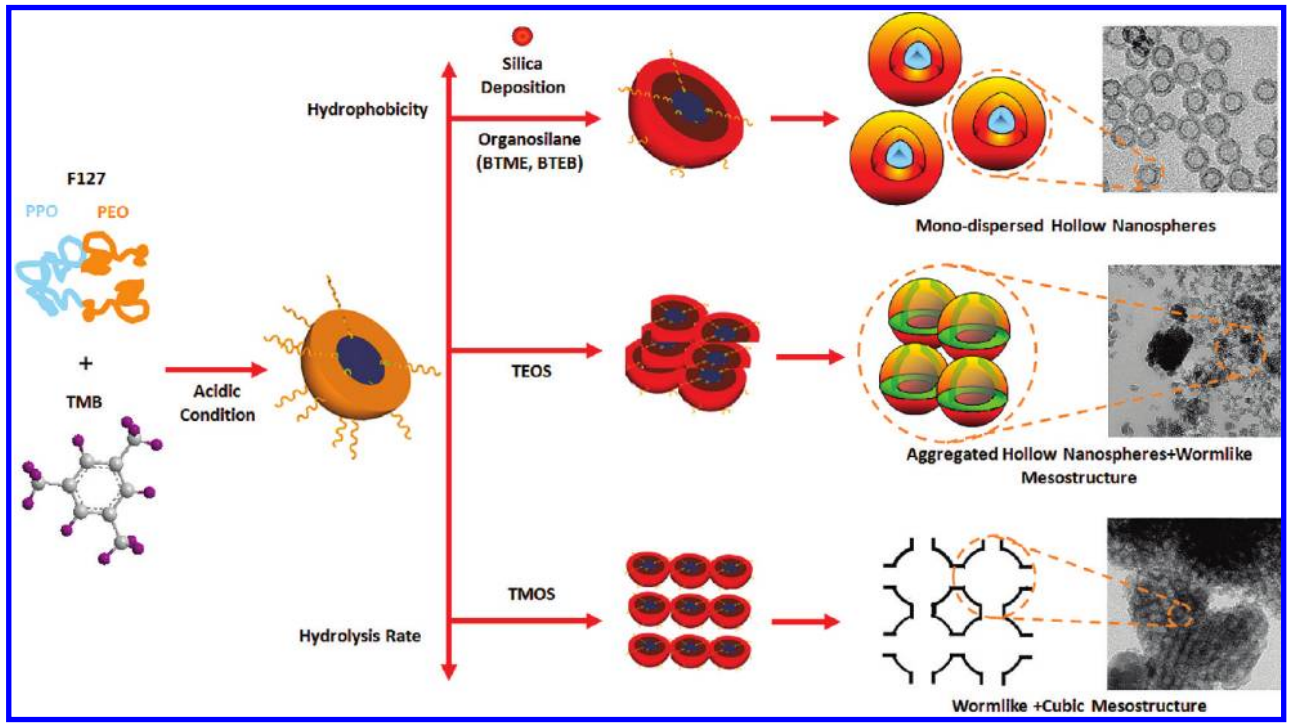

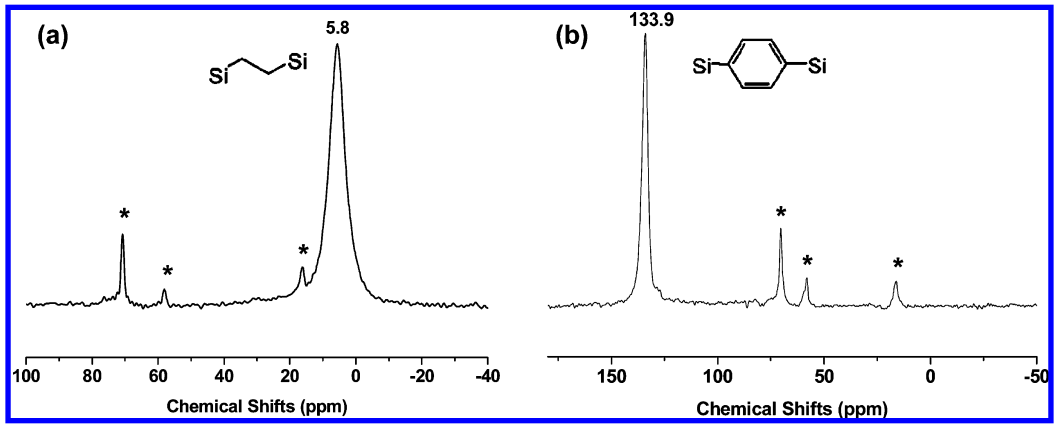

Figure 8. Solid-state ^{13}C CP MAS NMR spectra for organosilica hollow nanospheres (a) NES-0-105 and (b) NBS-*4*23-105.

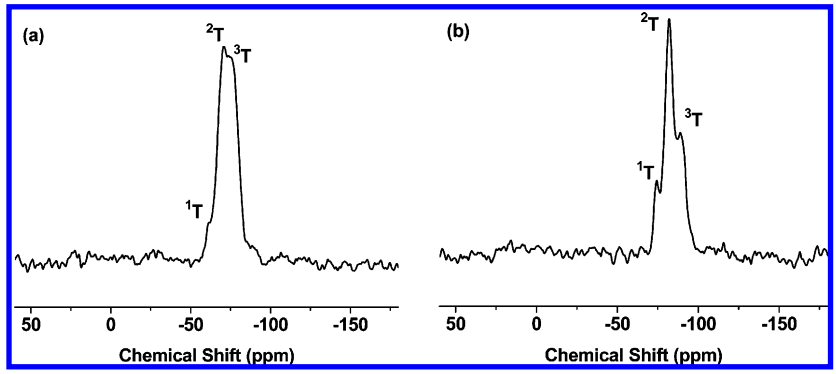

Figure 9. Solid-state ^{29}Si NMR spectra for organosilica hollow nanospheres (a) NES-0-105 and (b) NBS-423-105.

density on the surface of surfactant micelles was further decreased due to the penetration of TMB into the micelles, which may lead to dispersed single micelles and thus finally to highly dispersed hollow nanospheres. The fact that the particle size of OHNs decreases in the presence of a large amount of TMB is mainly due to the reorganization of the micelles. This occurs because TMB can exist both in the PPO core and outside the PPO core (Figure S6, Supporting Information).[35] With the addition of TMB molecules, the core size of the F127 micelle (Figure S6, Supporting Information) and the TMB molecules

are first located at the core of the micelles. In the presence of a large amount of TMB in the initial mixture, the repulsion of the hydrophilic PEO block and the hydrophobic TMB molecules makes more TMB molecules aggregate around the edge of the hydrophobic PPO core, and high-density TMB is formed around the edge (Figure S6, Supporting Information), which may cause a decrease of the particle size. A previous study indicated that the extended PEO groups play an important role in protecting the particles from agglomeration; the long PEO chains in F127 indeed function as a steric stabilizer to keep the particles from agglomeration even after silica is deposited.[13] As mentioned above, a large amount of TMB would make more TMB molecules aggregate around the edge of the hydrophobic PPO core and shorten the PEO chains, which leads to the worse dispersion of the resulting organosilica hollow nanospheres.

4. Conclusions

In summary, monodispersed organosilica hollow nanospheres (OHNs) with a particle size around 25 nm can be successfully synthesized by micelle templated coassembly of a triblock copolymer F127 [$(EO)_{106}(PO)_{70}(EO)_{106}$] surfactant with TMB and organosilane. The size and shell thickness of the OHNs could be controlled through adjusting the molar ratio of TMB/F127 in the initial mixture. To the best of our knowledge, benzene−silica hollow nanopsheres with a particle size of around 18 nm were synthesized for the first time under the current synthetic system. The organosilane precursors, such as BTME, BTEB, and BTSEB, favor the formation of hollow nanospheres. TMOS and TEOS tend to form mesostructured particles and a mixture of mesostructured particles and hollow nanospheres, respectively. The hydrophobicity and hydrolysis rate of the silane precursors play an important role in the structure and morphology formation of the resultant materials. Our studies indicate that OHNs with other functional groups could be successfully synthesized by finely tuning the hydrophobicity/hydrophilicity and hydrolysis rate of the silane precursor.

Acknowledgment. We are grateful for the financial support of the National Basic Research Program of China (2005CB221407, 2009CB623503) and Programme Strageties Scientific Alliances between China and the Netherlands (2008DFB50130). We are grateful to Prof. Mengfei Luo and Ms. Aiping Jia for HRSEM images from Zhejiang Normal University. The authors thank Mr. Fengtao Fan for his kind help in drawing the scheme.

Supporting Information Available: Table showing the preparation parameters and physicochemical properties of nanostructured silicas and figures showing high magnification SEM images, TEM images, XRD patterns, nitrogen adsorption and desorption isotherm curves, FT-IR spectra, and a schematic illustration of the location of TMB molecules in the expanded F127 micelles. This material is available free of charge via the Internet at http://pubs.acs.org.

References and Notes

(1) Loy, D. A.; Shea, K. J. Bridged Polysilsesquioxanes. Molecular Engineering of Hybrid Organic-Inorganic Materials. *MRS Bull.* **2001**, 368–376.

(2) Fujita, S.; Inagaki, S. Self-Organization of Organosilicas Solids with Molecular-Scale and Mesoscale Periodicities. *Chem. Mater.* **2008**, *20*, 891–908.

(3) Hoffmann, F.; Cornelius, M.; Morell, J.; Fröba, M. Silica-Based Mesoporous Organic-Inorganic Hybrid Materials. *Angew. Chem., Int. Ed.* **2006**, *45*, 3216–3251.

(4) Yuan, J. Y.; Xu, Y. Y.; Walther, A.; Bolisetty, S.; Schumacher, M.; Schmalz, H.; Ballauff, M.; Müller, A. H. E. Water-soluble Organosilica Hybrid Nanowires. *Nat. Mater.* **2008**, *7*, 718–722.

(5) Djojoputro, H.; Zhou, X. F.; Qiao, S. Z.; Wang, L. Z.; Yu, C. Z.; Lu, G. Q. Periodic Mesoporous Organosilica Hollow Spheres with Tunable Wall Thickness. *J. Am. Chem. Soc.* **2006**, *128*, 6320–6321.

(6) Liu, J.; Yang, Q. H.; Zhang, L.; Yang, H. Q.; Gao, J. S.; Li, C. Organic-inorganic Hybrid Hollow Nanospheres with Microwindows on the Shell. *Chem. Mater.* **2008**, *20*, 4268–4275.

(7) Tan, B.; Vyas, S. M.; Lehmler, H.-J.; Knutson, B. L.; Rankin, S. E. Synthesis of Inorganic and Organic-Inorganic Hybrid Hollow Particles Using a Cationic Surfactant with a Partially Fluorinated Tail. *Adv. Funct. Mater.* **2007**, *17*, 2500–2508.

(8) Zhou, X. F.; Qiao, S. Z.; Hao, N.; Wang, X. L.; Yu, C. Z.; Wang, L. Z.; Zhao, D. Y.; Lu, G. Q. Synthesis of Ordered Cubic Periodic Mesoporous Organosilicas with Ultra-Large Pores. *Chem. Mater.* **2007**, *19*, 1870–1876.

(9) Zhang, Y.; Yu, M. H.; Zhou, L.; Zhou, X. F.; Zhao, Q. F.; Li, H. X.; Yu, C. Z. Organosilica Multilamellar Vesicles with Tunable Number of Layers and Sponge-Like Walls via One Surfactant Templating. *Chem. Mater.* **2008**, *20*, 6238–6243.

(10) Qiao, S. Z.; Lin, C. X.; Jin, Y. G.; Li, Z.; Yan, Z. M.; Hao, Z. P.; Huang, Y. N.; Lu, G. Q. Surface-Functionalized Periodic Mesoporous Organosilica Hollow Spheres. *J. Phys. Chem. C* **2009**, *113*, 8673–8682.

(11) Gao, J. S.; Liu, J.; Bai, S. Y.; Wang, P. Y.; Zhong, H.; Yang, Q. H.; Li, C. The Nanocomposites of SO_3H-hollow-nanosphere and Chiral Amine for Asymmetric Aldol Reaction. *J. Mater. Chem.* **2009**, *19*, 8580–8588.

(12) Yuan, J. J.; Wan, D. C.; Yang, Z. L. A Facile Method for the Fabrication of Thiol-Functionalized Hollow Silica Spheres. *J. Phys. Chem. C* **2008**, *112*, 17156–17160.

(13) Huo, Q.; Liu, J.; Wang, L.-Q.; Jiang, Y.; Lambert, T. N.; Fang, E. A New Class of Silica Cross-Linked Micellar Core-Shell Nanoparticles. *J. Am. Chem. Soc.* **2006**, *128*, 6447–6453.

(14) Yuan, J. J.; Mykhaylyk, O. O.; Ryan, A. J.; Armes, S. P. Cross-Linking of Cationic Block Copolymer Micelles by Silica Deposition. *J. Am. Chem. Soc.* **2007**, *129*, 1717–1723.

(15) Khanal, A.; Inoue, Y.; Yada, M.; Nakashima, K. Synthesis of Silica Hollow Nanoparticles Templated by Polymeric Micelle with Core-Shell-Corona Structure. *J. Am. Chem. Soc.* **2007**, *129*, 1534–1535.

(16) Shea, K. J.; Loy, D. A.; Webster, O. Arylsilsesquioxane Gels and Related Materials. New Hybrids of Organic and Inorganic Networks. *J. Am. Chem. Soc.* **1992**, *114*, 6700–6710.

(17) Wang, H.; Wang, Y.; Zhou, X.; Zhou, L.; Tang, J.; Lei, J.; Yu, C. Z. Siliceous Unilamellar Vesicles and Foams by Using Block-Copolymer Cooperative Vesicle Templating. *Adv. Funct. Mater.* **2007**, *17*, 613–617.

(18) Inagaki, S.; Guan, S.; Ohsuna, T.; Terasaki, O. An Ordered Mesoporous Organosilica Hybrid Material with a Crystal-like Wall Structure. *Nature* **2002**, *416*, 304–307.

(19) Yang, Q. H.; Liu, J.; Yang, J.; Kapoor, M. P.; Inagaki, S.; Li, C. Synthesis, characterization, and catalytic activity of sulfonic acid-functionalized periodic mesoporous organosilicas. *J. Catal.* **2004**, *228*, 265–272.

(20) Goto, Y.; Inagaki, S. Synthesis of large-pore phenylene-bridged mesoporous organosilica using triblock copolymer surfactant. *Chem. Commun.* **2002**, 2410–2411.

(21) Kapoor, M. P.; Yang, Q. H.; Inagaki, S. Organization of Phenylene-Bridged Hybrid Mesoporous Silisesquioxane with a Crystal-like Pore Wall from a Precursor with Nonlinear Symmetry. *Chem. Mater.* **2004**, *16*, 1209–1213.

(22) Yang, Q.; Kapoor, M. P.; Inagaki, S. Sulfuric Acid-Functionalized Mesoporous Benzene-Silica with a Molecular-Scale Periodicity in the Walls. *J. Am. Chem. Soc.* **2002**, *124*, 9694–9695.

(23) Ohashi, M.; Kapoor, M. P.; Inagaki, S. Chemical modification of crystal-like mesoporous phenylene-silica with amino group. *Chem. Commun.* **2008**, 841–843.

(24) Fan, J.; Yu, C. Z.; Gao, F.; Lei, J.; Tian, B. Z.; Wang, L. M.; Luo, Q.; Tu, B.; Zhou, W. Z.; Zhao, D. Y. Cubic Mesoporous Silica with Large Controllable Entrance Sizes and Advanced Adsorption Properties. *Angew. Chem., Int. Ed.* **2003**, *42*, 3146–3150.

(25) Fan, J.; Yu, C. Z.; Lei, J.; Zhang, Q.; Li, T. C.; Tu, B.; Zhou, W. Z.; Zhao, D. Y. Low-Temperature Strategy to Synthesize Highly Ordered Mesoporous Silicas with Very Large Pores. *J. Am. Chem. Soc.* **2005**, *127*, 10794–10795.

(26) Bao, X. Y.; Li, X.; Zhao, X. S. Synthesis of Large-pore Methylene-bridged Periodic Mesoporous Organosilicas and Its Implications. *J. Phys. Chem. B* **2006**, *110*, 2656–2661.

(27) Burleigh, M. C.; Markowitz, M. A.; Spector, M. S.; Gaber, B. P. Porous Polysilsesquioxanes for the Adsorption of Phenols. *Environ. Sci. Technol.* **2002**, *36*, 2515–2518.

(28) Li, C. M.; Liu, J.; Shi, X.; Yang, J.; Yang, Q. H. Periodic Mesoporous Organosilicas with 1,4-Diethylenebenzene in the Mesoporous Wall: Synthesis, Characterization, and Bioadsorption Properties. *J. Phys. Chem. C* **2007**, *111*, 10948–10954.

(29) Tan, B.; Rankin, S. E. Study of the Effects of Progressive Changes in Alkoxysilane Structure on Sol-Gel Reactivity. *J. Phys. Chem. B* **2006**, *110*, 22353–22364.

(30) Brinker, C. J. Hydrolysis and Condensation of Silicates: Effect on Structure. *J. Non-Cryst. Solids* **1988**, *100*, 31–50.

(31) Hook, R. J. A ^{29}Si NMR study of the sol-gel polymerisation rates of substituted ethoxysilanes. *J. Non-Cryst. Solids* **1996**, *195*, 1–15.

(32) Zhu, G. R.; Yang, Q. H.; Zhong, H.; Jiang, D. M.; Li, C. A Potential Chiral Stationary Phases: Phase Transformation of the Periodic Mesoporous Organosilicas Assisted by Organotrialkoxysilane. *J. Phys. Chem. B* **2007**, *111*, 8027–8033.

(33) Yu, C. Z.; Tian, B. Z.; Fan, J.; Stucky, G. D.; Zhao, D. Y. Salt Effect in the Synthesis of Mesoporous Silica Templated by Non-ionic Block Copolymers. *Chem. Commun.* **2001**, 2726–2727.

(34) Guo, W. P.; Park, J.-Y.; Oh, M.-O.; Jeong, H.-W.; Cho, W.-J.; Kim, I.; Ha, C.-S. Triblock Copolymer Synthesis of Highly Ordered Large-Pore Periodic Mesoporous Organosilicas with the Aid of Inorganic Salts. *Chem. Mater.* **2003**, *15*, 2295–2298.

(35) Yuan, S.-L.; Zhang, X.-Q.; Chan, K.-Y. Effects of Shear and Charge on the Microphase Formation of P123 Polymer in the SBA-15 Synthesis Investigated by Mesoscale Simulations. *Langmuir* **2009**, *25*, 2034–2045.

(36) Tang, J.; Zhou, X.; Zhao, D.; Lu, G. Q.; Zou, J.; Yu, C. Hard-Sphere Packing and Icosahedral Assembly in the Formation of Mesoporous Materials. *J. Am. Chem. Soc.* **2007**, *129*, 9044–9048.

JP909931Z